Optical measurement of Cs distribution in the large negative ion source[a)]

K. Ikeda, K. Nagaoka, and Y. Takeiri
National Institute for Fusion Science, 322-6 Oroshi, Toki, Gifu 509-5292, Japan

U. Fantz
Max-Planck-Institut fuer Plasmaphysik, EURATOM Association, D-85748 Garching, Germany

O. Kaneko, M. Osakabe, Y. Oka, and K. Tsumori
National Institute for Fusion Science, 322-6 Oroshi, Toki, Gifu 509-5292, Japan

(Presented 29 August 2007; received 28 August 2007; accepted 26 October 2007; published online 7 February 2008)

To investigate a Cs behavior, optical diagnostic tools have been installed in the large negative ion source, an arc discharge used at large helical device neutral beam injector. A large Cs sputtering is observed during beam extraction due to the backstreaming H^+ ions. Distribution of Cs^+ light is uniform in the case of a balanced arc discharge, but large increase of Cs^+ light during beam extraction is observed in a nonuniform arc discharge. Controlling of the discharge uniformity is effective to reduce the local heat loading from the backstreaming H^+ ions at the backplate of ion source. © *2008 American Institute of Physics.* [DOI: 10.1063/1.2816958]

I. INTRODUCTION

The cesium (Cs) assisted enhancement of hydrogen (H) or deuterium (D) negative ions brought a drastic breakthrough to develop negative ion sources for high energy neutral beam injectors (NBIs). Using the Cs effect, H^- or D^- ion sources for NBI have been built in many facilities.[1–3] For the future NBI system at the fusion experiment ITER,[4] optimization of the Cs conditions and Cs distribution in negative ion source are key issues.

At the large helical device (LHD), three H^- based NBI systems have been installed now. We have successfully operated the high power NBI by using filament-arc discharge.[1] Recently, the optical diagnostic technique has been established to investigate the Cs dynamics and negative ion production inside the rf ion source at IPP, Garching.[5] However, the relation between the beam profile and the distribution of cesium in the large-scale ion source has not been determined. In order to investigate the behavior of Cs distribution in the large negative ion source by using arc discharge, we have installed the optical diagnostic tools on the LHD-NBI source.[6] Experiments have been carried out to demonstrate Cs evaporation by backstreaming positive ions and Cs distributions in uniform and nonuniform discharges.

II. EXPERIMENTAL APPARATUS

Figure 1 shows a schematic view of the optical configuration on the LHD-NBI source. The inner sizes of the arc chamber are 1450 mm in height (y axis), 350 mm in width (x axis), and 223 mm in depth (z axis) from the backplate surface to the plasma grid (PG). Three Cs ovens are equipped on the backplate of the arc chamber. Arc discharge distribution is controlled by 12 units of filament and arc power supplies.[7] There are four line of sights (LOSs) from the backplate port perpendicular to the plasma grid. Each LOS is arranged at $y=435$ mm, $y=87$ mm, $y=-87$ mm, and $y=-435$ mm, respectively.[6] We have arranged the low resolution (1.5 nm) survey spectrometer (PLASUS EmiCon system) to take many spectra simultaneously from 200 to 870 nm, and the high resolution (0.12 nm) spectrometer (ANDOR Shamrock system) with charge coupled device (CCD) detector with the size of 1024 pixels in width and 256 pixels in height to take close-up spectra into the 35 nm narrow wavelength range.

We have also installed a beam profile monitor in front of the neutralizer where it is 2.2 m downstream from the ground grid.[7] This system consists of the interline transfer CCD camera (Panasonic WV-BP70) coupled with the H_α bandpass filter (Andover 656FS10-25). The extracted beam distribution in the vertical direction is estimated from the H_α profile.

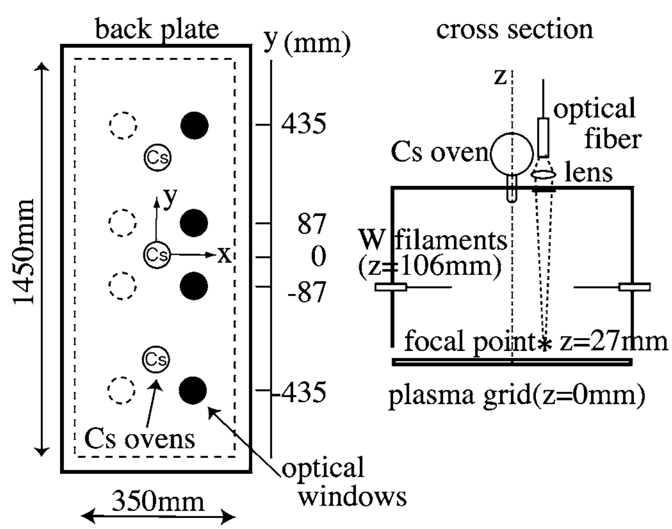

FIG. 1. Schematic view of the optical configuration in the LHD-NBI arc discharge source. Four optical LOSs are set perpendicular to the plasma grid.

[a)]Contributed paper, published as part of the Proceedings of the 12th International Conference on Ion Sources, Jeju, Korea, August 2007.

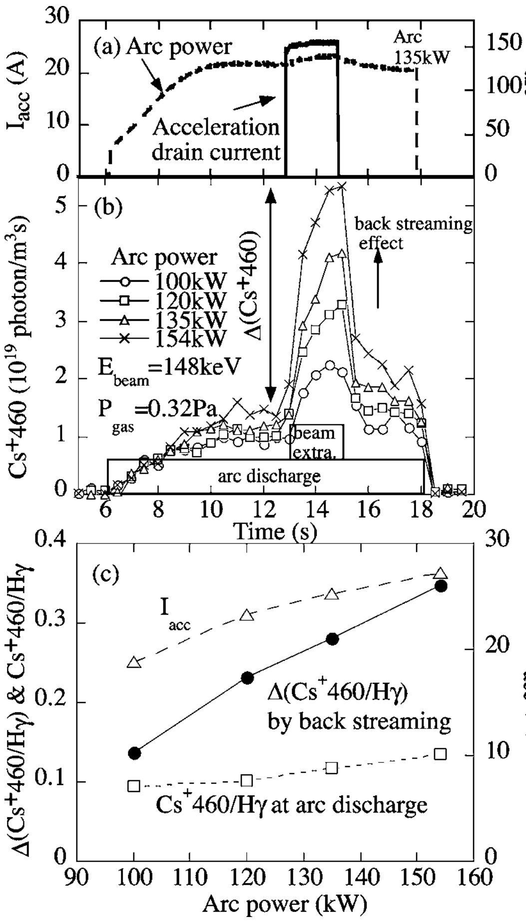

FIG. 2. Time traces of the arc discharge power, the acceleration drain current (a), and Cs^+ light (b). The discharge power dependences of the increase of the Cs^+ light normalized by H_γ with and without beam extraction (closed and open circles, respectively) and the acceleration drain current (open triangles) are shown in (c).

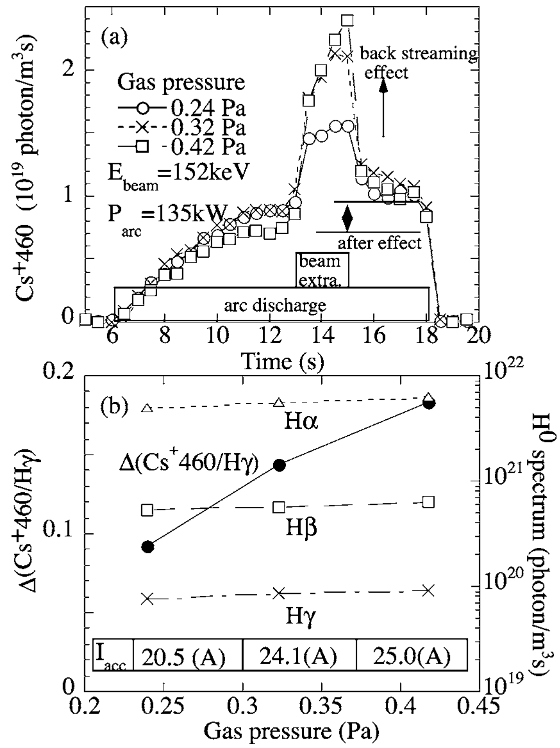

FIG. 3. Time trace of the Cs^+ light at different gas pressures (a). (b) shows the pressure dependence of the increase of the Cs^+ light during beam extraction (closed circles), neutral hydrogen light ($H_\alpha, H_\beta, H_\gamma$), and acceleration drain currents (table).

III. Cs EVAPORATION BY BACKSTREAMING POSITIVE IONS

In our arc discharge source, we have observed the hydrogen Balmer spectra ($H_\alpha, H_\beta, H_\gamma$), the molecular hydrogen Fulcher spectra (600–630 nm), the neutral Cs^0 spectrum (852 nm), the ion Cs^+ spectra (460 and 522 nm), the impurity oxygen spectra (777 nm), and the continuum spectrum originating from tungsten (W) filaments. The Cs^+ spectrum is stronger than the Cs^0 spectrum, which means that more than 99% of the Cs is ionized in arc discharge plasma.[6] We have not observed the W^0 spectrum around 400 nm, which is different from the result in the KAMABOKO-III source at CEA.[8]

Figure 2(a) shows time trace of the arc power (P_{arc}) and the acceleration drain current (I_{acc}); here the horizontal axis is the elapsed time since it turns on the filament power supplies. The arc voltage is applied at $t=6$ s to $t=18$ s, and the beam extraction voltage is also applied at $t=13$ s to $t=15$ s. During the beam extraction, the I_{acc} small increases are similar to the P_{arc} because of the increasing thermal electrons from W filaments by the heat load of backstreaming ions. Figure 2(b) shows time traces of the Cs^+ light for various arc powers. Without beam extraction, the Cs^+ light intensity small increases show increasing arc power, since Cs evaporates from the arc chamber wall due to the heat load by arc discharge. During beam extraction, large increase of the Cs^+ light appears although stable discharge condition is given, the latter represented by constant hydrogen light (H_α, H_β, and H_γ). Increase of the Cs^+ light indicates an increase of cesium ions inside of arc plasma. The I_{acc} does not increase so during beam extraction with the large increasing Cs^+ light signals, since the perpendicular LOS mainly measures the Cs spectrum in the discharge area. To obtain the relation of Cs light intensity and H^- production by the surface effect, a LOS near the plasma grids will be needed.

Additional Cs sputtering from the surface of the backplate of the arc chamber is produced by the impact of backstreaming positive ions. The same behavior was observed in other negative ion sources.[5,9] At the beginning of the beam extraction, we have observed more intense and rapid increase of the Cs light than that of Refs. 5 and 9. We have clearly observed that the additional Cs sputtering depends on the arc discharge power during otherwise stable plasma condition, as shown in Fig. 2(c); here, the additional Cs^+ light written as $\Delta(Cs^+460/H_\gamma)$ is normalized by the H_γ light which well reflects a plasma condition at discharge power and filling gas pressure. At increasing arc power, the extraction beam current and the additional Cs sputtering increase. The extraction voltage is fixed in this case. The occasion of such rapid increase is not only the high extraction voltage (148 kV) but also the high H^- beam current most likely.

We have also observed the increase of Cs sputtering by increasing hydrogen gas pressure at a constant 135 kW arc power and a 152 keV beam energy, as shown in Fig. 3. The extraction current increases at increasing gas pressure, and it

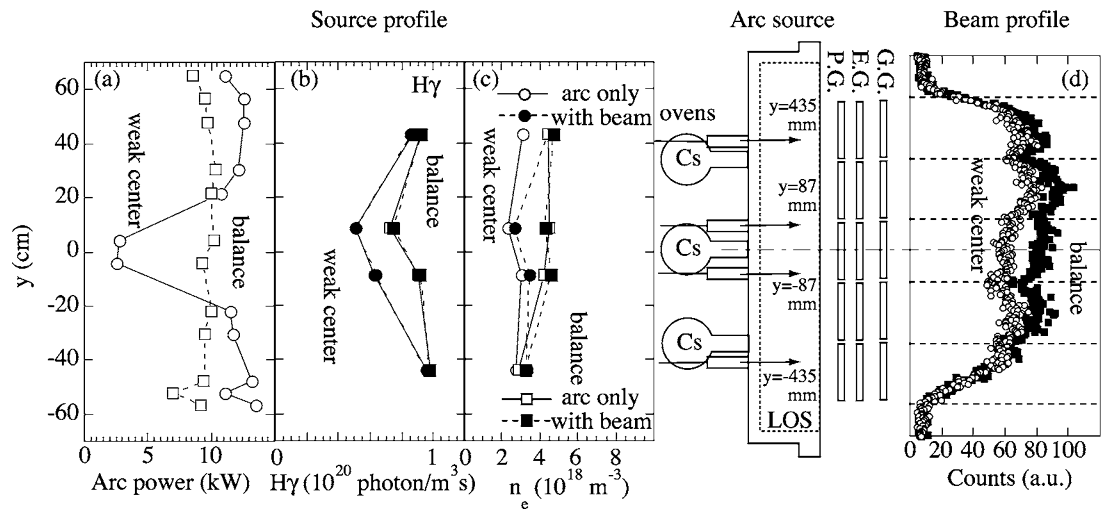

FIG. 4. Distribution of the applied arc discharge power in the balanced discharge and the weak center discharge (a). The profiles of H_γ light (b) and the electron density (c) are consistent with the discharge distribution. (d) shows the extracted beam profile estimated by H_α distribution.

is saturated in the higher gas pressure discharge. The $\Delta(Cs^+460/H_\gamma)$ increases strongly though the I_{acc} is saturated in the high pressure discharge, as shown in Fig. 3(b). This behavior indicates that the neutral hydrogen density also influences the production of backstreaming ions. At the surface of the backplate, we have seen that the backstreaming spots are of the same size as those of the PG hole (ϕ=14 mm). This clear spot seems a good focus condition for the backstreaming H^+. So the backstream H^+ ion, which is produced around the grounded grid due to the interaction of the neutral hydrogen and accelerated beam most likely, goes back into the arc source along the same route of the beam extraction with an opposite direction. At present, the influence with H^+ backstream is not serious on our arc sources. It is likely a high heat flux on the back side component such as a filament in an arc source and a rf driver in a rf source by extracting a negative ion beam with higher energy and higher current in a future NBI.

IV. Cs DISTRIBUTION IN NONUNIFORM DISCHARGE

Figure 4 shows the two different arc discharge distributions and the extracted beam distributions along the vertical axis. One case is the balanced arc discharge with a 112 kW total arc power, as shown by the square marks in (a), and it produces the uniform beam, as shown in (d). The other case is the weak discharge at the center position with a total of 125 kW arc power, as shown by the circle marks in Fig. 4(a). The gas pressure (0.3 Pa) and beam energy (148 keV) are the same. The arc voltages and the arc currents at the two center circuits drop to 60% and 40% from the other circuits, respectively. The filament voltage and current are of the same condition in two cases. At the center weak discharge, H_γ light and electron density also decrease in the center part, as shown in Figs. 4(b) and 4(c); here electron densities are obtained from the ratio of H_β/H_γ.[5] This decrease is not so much to the arc power distribution (~60%), because the center part of the electrons is recovered by the drift motion of electrons in the bottom area due to the magnetic filter field. The density distributions during only arc discharge and during beam extraction are almost the same. It has little influence on the discharge distribution and the H_γ intensity by backstreaming ions. The beam distribution estimated by the H_α light intensity also decreases at the center grid in the weak center discharge, as shown in Fig. 4(d). This result is consistent with the source plasma distribution.

On the other hand, an interesting behavior appears on the Cs^+ light distribution. In the case of the balanced discharge, Cs^+ light distribution forms a flat profile during both arc discharge and beam extraction, as shown in Fig. 5(a). The additional Cs^+ light $\Delta(Cs^+460/H_\gamma)$ is also balanced, as shown the square marks in Fig. 5(c). That means the Cs sputtering on the backplate due to the backstreaming H^+ ions is uniform along the vertical axis of arc source. In the weak center discharge, Cs^+ light intensities become weak at the top and bottom regions, as shown in Fig. 5(b). There is intense Cs^+ light at the center of two LOSs during the beam extraction. Such nonuniform Cs^+ light during beam extraction is inconsistent with the hollow beam distribution shown in Fig. 4. The drain beam currents I_{acc} in balance discharge and weak center discharge are 18.8 and 16.4 A, respectively. This current ratio corresponds to the summation of the beam profile. The summation of the $\Delta(Cs^+460/H_\gamma)$ in the weak center discharge, however, is larger than that in the balance discharge, as shown by the circle marks in Fig. 5(c).

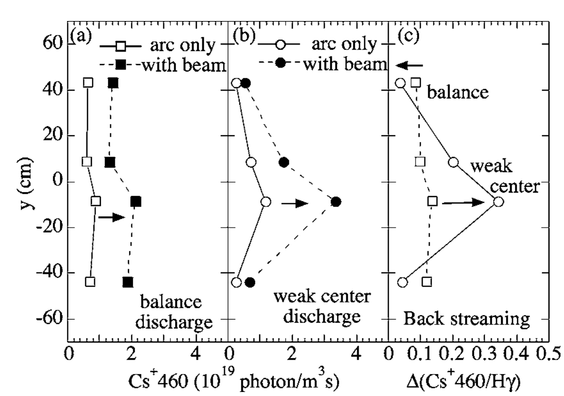

FIG. 5. Profiles of the Cs^+ light in the balanced discharge (a) and the weak center discharge (b). Additional Cs sputtering due to the backstreaming H^+ ions increases at the center (c).

To check the local deposition of Cs on the backplate at the nonuniform discharge, we set the balance discharge again immediately after the weak center discharge. It is also observed that the flat distribution of Cs^+ light is the same as that of Fig. 5(a). So the local deposition of Cs on the backplate can be excluded.

On the other hand, a small Cs accumulation occurs at the center during only arc discharge with static state, as shown by the open circles in Fig. 5(b). If it is caused by the hollow plasma distribution, Cs accumulation ratio during the beam extraction has to be same as that during only arc discharge. So the effect of Cs accumulation might be not so much.

This nonuniform Cs distribution occurs by only changing the discharge distribution. If the reason is not a cesium accumulation, it is caused by the production of the backstream ions around the ground grids. The production of the backstreaming H^+ ions is related to the neutral hydrogen density. If the neutral hydrogen distribution forms peaked profile due to the hollow beam pressure distribution, then an intense backstreaming might occur.

In conclusion, the nonuniform backstreaming has been observed in the large negative ion source. This distribution is inconsistent with the source discharge distribution. Conclusive proof of this behavior is not determined now, but the improved beam uniformity is advantageous for decreasing the backstreaming ions.

ACKNOWLEDGMENTS

The authors would like to thank the technical staff for their effort in supporting the NBI operations. This work is supported by NIFS07ULBB501. Also, this work is supported by the program of Japan Society for the Promotion of Science Bilateral Joint Projects and Seminars 2006.

[1] Y. Takeiri, O. Kaneko, K. Tsumori, Y. Oka, K. Ikeda, M. Osakabe, K. Nagaoka, E. Asano, T. Kondo, M. Sato, and M. Shibuya, Nucl. Fusion **46**, S199 (2006).
[2] E. Speth, H. D. Falter, P. Franzen, U. Fantz, M. Bandyopadhyay, S. Christ, A. Encheva, M. Fröschle, D. Holtum, B. Heinemann, W. Kraus, A. Lorenz, Ch. Martens, P. McNeely, S. Obermayer, R. Riedl, R. Süss, A. Tanga, R. Wilhelm, and D. Wünderlich, Nucl. Fusion **46**, S220 (2006).
[3] Y. Ikeda, N. Umeda, N. Akino, N. Ebisawa, L. Grisham, M. Hanada, A. Honda, T. Inoue, M. Kawai, M. Kazawa, K. Kikuchi, M. Komata, K. Mogaki, K. Noto, F. Okano, T. Ohga, K. Oshima, T. Takenouchi, Y. Tanai, K. Usui, H. Yamazaki, and T. Yamamoto, Nucl. Fusion **46**, S211 (2006).
[4] ITER Technical Basis, 2002 ITER EDA Documentation Series No. 24, International Atomic Energy Agency (IAEA).
[5] U. Fantz, H. Falter, P. Franzen, D. Wünderlich, M. Berger, A. Lorenz, W. Kraus, P. McNeely, R. Riedl, and E. Speth, Nucl. Fusion **46**, S297 (2006).
[6] K. Ikeda, U. Fantz, K. Nagaoka, Y. Takeiri, M. Osakabe, K. Tsumori, O. Kaneko, and Y. Oka, Plasma Fusion Res. **2**, S1047 (2007).
[7] K. Ikeda, Y. Takeiri, O. Kaneko, K. Nagaoka, Y. Oka, M. Osakabe, K. Tsumori, M. Sato, E. Asano, and T. Kawamoto, Rev. Sci. Instrum. **75**, 1744 (2004).
[8] U. Fantz, H. D. Falter, P. Franzen, E. Speth, R. Hemsworth, D. Boilson, and A. Krylov, Rev. Sci. Instrum. **77**, 03A516 (2006).
[9] A. Krylov, D. Boilson, U. Fantz, R. S. Hemsworth, O. Provitina, S. Pontremoli, and B. Zaniol, Nucl. Fusion **46**, S324 (2006).